Molecular and Electronic Structure in the Metal-to-Ligand Charge-Transfer Excited States of d^6 Transition-Metal Complexes in Solution

Jonathan V. Caspar,[†] T. David Westmoreland,[†] George H. Allen,[†] Paul G. Bradley,[‡] Thomas J. Meyer,*[†] and William H. Woodruff*[‡]

Contribution from the Departments of Chemistry, The University of North Carolina, Chapel Hill, North Carolina 27514, and The University of Texas at Austin, Austin, Texas 78712.
Received July 7, 1983

Abstract: The ground and metal-to-ligand (MLCT) excited electronic states of the complexes $Os(bpy)_n(P_2)_{3-n}^{2+}$ (bpy = 2,2′-bipyridine, P_2 = *cis*-$(C_6H_5)_2PCH{=}CHP(C_6H_5)_2$; n = 1-3) have been studied by resonance Raman spectroscopy, time-resolved resonance Raman spectroscopy, and emission spectroscopy. The time-resolved resonance Raman evidence confirms that the charge-transfer electron density is localized in the lowest π^* orbital of one bpy ligand rather than delocalized over the π^* orbitals of all of the available bpy ligands on the vibrational time scale. The amount of charge transferred from the metal to bpy π^* in the MLCT state has been determined. Application of Badger's rule to the Raman data and Franck-Condon analysis of the emission data lead to two independent determinations of average bond length displacements in the MLCT state. The two approaches yield displacement values that agree within 0.001-0.003 Å for the three complexes studied, suggesting that it may be possible to determine excited-state structures in solution with a precision similar to that of a good X-ray crystal structure. Analysis of time-resolved resonance Raman and emission data for $Ru(bpy)_3^{2+}$, $Ru(bpy)_2(en)^{2+}$, and *fac*-$Re(bpy)(CO)_3Cl$ by these methods yields results in agreement with the osmium data. The results suggest a general prescription for the determination of the molecular and electronic structures of electronically excited states in solution.

As photochemical systems in solution, the metal-to-ligand charge-transfer (MLCT) excited states of d^6 transition-metal complexes are rapidly becoming a paradigm. Information has appeared detailing both the photochemical and photophysical properties of many such systems.[1-8] However, to date, essentially no quantitative information has emerged concerning molecular structure in this class of excited state in fluid solution. In this report we describe a study of this kind on the emitting MLCT excited states for the series of complexes $Os(bpy)_n(P_2)_{3-n}^{2+}$ (bpy = 2,2′-bipyridine, P_2 = *cis*-1,2-bis(diphenylphosphino)ethylene (*cis*-$Ph_2PCH{=}CHPPh_2$); n = 1-3), which appear to be largely triplet in character but which contain considerable single character via spin-orbit coupling. The bases for our studies include both emission bandshape analyses and time-resolved resonance Raman spectroscopy. The results obtained allow us to infer quantitative information concerning both electronic and molecular structures for the MLCT excited states.

Previously, time-resolved resonance Raman studies[9-11] have conclusively established that the realistic formulation of the 600-ns-lived MLCT state of $Ru(bpy)_3^{2+}$ is $Ru^{III}(bpy)_2(bpy^{-\cdot})^{2+}$; i.e., the MLCT electron density is localized on a single bpy ligand on the time scale of molecular vibrations. This possibility had been suggested previously[1a,2] and has since been supported by several lines of evidence from a number of laboratories.[6,7,8b,10,11]

The experimental approaches employed in this study extend the conclusions concerning localization in MLCT excited states to the Os complexes and allow several additional issues to be explored. One issue is an estimation of the extent of charge transfer to the ligand(s) in the MLCT state and the relationship of the extent of charge transfer to the $d\pi-\pi^*$ energy gap as reflected by absorption or emission spectra. A second issue is the relationship beween the electronic spectra of the ground and excited states and their vibrational spectra. Finally, and most significantly, we have been able to estimate structural changes between the ground and excited states in a self-consistent way both from Franck-Condon analyses of emission bandshapes and from Raman frequency shifts. The agreement between the two approaches with regard to structural differences between ground and excited states is gratifying. More importantly, given that our methods are potentially applicable to a wide variety of systems, they suggest a general approach to the analyses of molecular and electronic structures of excited states in solution.

Experimental Section

Preparation of Complexes. $Os(bpy)_3(PF_6)_2$ and $Os(bpy)_2(cis\text{-}Ph_2PCH{=}CHPPh_2)(PF_6)_2$ were prepared according to the method of Kober et al.[12a] $Os(bpy)(cis\text{-}Ph_2PCH{=}CHPPh_2)_2(PF_6)_2$ was prepared from $Os(bpy)Cl_4$ by Sullivan et al.[12b] All compounds were purified by column chromatography on neutral alumina, using an acetonitrile-toluene mixture as eluant.

Emission Spectra and Spectral Fits. Corrected emission spectra were obtained in 4:1 EtOH/MeOH glasses at 77 K with a SLM Instruments, Inc., Model 8000 photon-counting fluorimeter. Spectral fits of the low-temperature emission spectra were made by using a modified version of the two-mode fitting program described earlier.[13] The equations used

[†] The University of North Carolina.
[‡] The University of Texas at Austin.

(1) (a) DeArmond, M. K. *Acc. Chem. Res.* **1974**, *7*, 309. (b) DeArmond, M. K.; Carlin, C. M. *Coord. Chem. Rev.* **1981**, *36*, 325. (c) Kalyanasundaram, K. *Ibid.* **1982**, *46*, 159.
(2) (a) Sutin, N.; Creutz, C. *Adv. Chem. Ser.* **1978**, *No. 138*, 1. (b) Crosby, G. A. *Acc. Chem. Res.* **1975**, *8*, 231.
(3) (a) Meyer, T. J. *Acc. Chem. Res.* **1978**, *11*, 94; (b) *Prog. Inorg. Chem.* **1983**, *30*, 389.
(4) Balzani, V.; Bolletta, F.; Gandolfi, M. T.; Maestri, M. *Top. Curr. Chem.* **1978**, *75*, 1.
(5) (a) Hagar, G. D.; Crosby, G. A. *J. Am. Chem. Soc.* **1975**, *97*, 7031. (b) Hagar, G. D.; Watts, R. J.; Crosby, G. A. *Ibid.* **1975**, *97*, 7037. (c) Hipps, K. W.; Crosby, G. A. *Ibid.* **1975**, *97*, 7042. (d) Crosby, G. A.; Elfring, W. H., Jr. *J. Phys. Chem.* **1976**, *80*, 2206. (e) Pankuch, B. J.; Lacky, D. E.; Crosby, G. A. *Ibid.* **1980**, *84*, 2061. (f) Lacky, D. E.; Pankuch, B. J.; Crosby, G. A. *Ibid.* **1980**, *84*, 2068.
(6) (a) Felix, F.; Ferguson, J.; Gudel, H. U.; Ludi, A. *Chem. Phys. Lett.* **1979**, *62*, 153. (b) Felix, F.; Ferguson, J.; Gudel, H. U.; Ludi, A. *J. Am. Chem. Soc.* **1980**, *102*, 4096. Decurtins, S.; Felix, F.; Ferguson, J.; Gudel, H. U.; Ludi, A. *Ibid.* **1980**, *102*, 4102.
(7) Hipps, K. W. *Inorg. Chem.* **1980**, *19*, 1390.
(8) (a) Kober, E. M.; Meyer, T. J. *Inorg. Chem.* **1982**, *21*, 3967. (b) Kober, E. M.; Sullivan, B. P.; Meyer, T. J. *Ibid.*, in press.
(9) (a) Dallinger, R. F.; Woodruff, W. H. *J. Am. Chem. Soc.* **1979**, *101*, 4391. (b) Bradley, P. G.; Kress, N.; Hornberger, B. A.; Dallinger, R. F.; Woodruff, W. H. *Ibid.* **1981**, *103*, 7441.
(10) Forster, M.; Hester, R. E. *Chem. Phys. Lett.* **1981**, *81*, 42.
(11) Smothers, W. K.; Wrighton, M. S. *J. Am. Chem. Soc.* **1983**, *105*, 1067.
(12) (a) Kober, E. M.; Caspar, J. V.; Sullivan, B. P.; Meyer, T. J., manuscript in preparation. (b) Sullivan, B. P.; Caspar, J. V.; Meyer, T. J., manuscript in preparation.
(13) (a) Caspar, J. V. Ph.D. Thesis, The University of North Carolina, Chapel Hill, NC, 1982. (b) Allen, G. H.; White, R.; Rillema, D. P.; Meyer, T. J. *J. Am. Chem. Soc.* **1984**, *106*, 2613.

0002-7863/84/1506-3492$01.50/0

for fitting were of the form given in eq 1 and 2 and are discussed in detail

$$I(\bar{\nu}) = \sum_{v_M}\sum_{v_L} I_{v_M v_L}(\bar{\nu}) \quad (1)$$

$$I_{v_M v_L}(\bar{\nu}) = \left(\frac{\bar{\nu}_{00} - v_M\bar{\nu}_M - v_L\bar{\nu}_L}{\bar{\nu}_{00}}\right)^4 \left(\frac{S_M{}^{v_M}}{v_M!}\right)\left(\frac{S_L{}^{v_L}}{v_L!}\right) \times \left\{\exp\left[-4(\ln 2)\left(\frac{\bar{\nu} - \bar{\nu}_{00} + v_M\bar{\nu}_M + v_L\bar{\nu}_L}{\bar{\nu}_{1/2}}\right)^2\right]\right\} \quad (2)$$

in the appendix. In the equations v_M and v_L are the vibrational quantum numbers for high- (ν_M) and low-frequency (ν_L) vibrational progressions—the acceptor modes. The summation was carried out over 11 levels of vibrations ν_M and ν_L ($v = 0 \rightarrow 10$). With respect to eq 1 and 2, six spectral parameters were used in fitting the emission spectra. S_M and S_L are the vibrational coupling parameters, which are the objective of the computation and which are related to the distortion in the molecular coordinates corresponding to the high-frequency ($\bar{\nu}_M$, 1300–1450 cm^{-1}) and low-frequency ($\bar{\nu}_L$, ca. 400 cm^{-1}) acceptor modes (see Discussion). $\bar{\nu}_M$ and $\bar{\nu}_L$ are the wavenumbers of the acceptor modes; $\bar{\nu}_M$ is obtained from the spectral fits and is near the observed spacings in the 77 K emission spectrum and $\bar{\nu}_L$ is taken as a typical metal–ligand stretching frequency—the fits are relatively independent of the value chosen for $\bar{\nu}_L$ (±100 cm^{-1}). $\bar{\nu}_{00}$ is the wavenumber corresponding to the emission energy for the $v^* = 0 \rightarrow v = 0$ vibrational component of the emission progression, which is determined by the fits, and $\bar{\nu}_{1/2}$ is the full width at half-maximum of the 0–0 vibrational component of the emission, which is also determined in the fits.

For purposes of spectral fitting the emission spectra were converted from having abscissa linear in wavelength, which is a characteristic of the emission spectrometer used, to an abscissa linear in energy by the method of Parker and Rees[15] and as described in an earlier publication.[13b] We thank Professor James Demas for bringing this correction to our attention.

Resonance Raman and Time-Resolved Resonance Raman Spectroscopy. Resonance Raman spectra were obtained by using a SPEX Ramalog EU spectrometer with a RCA C31034A photomultiplier tube. Spectra using CW laser excitation (Spectra-Physics 171 Kr^+ or Ar^+ lasers) were detected by an Ortec 9300 Series photon counter. When pulsed laser excitation (Quanta-Ray DCR-1A Nd:YAG laser) was employed, a PAR 162 boxcar averager with a Model 165 gated integrator was used to detect the photomultiplier tube signal. Data were processed by using a Nicolet 1180E Raman data system. Solvents employed for the resonance Raman samples were H_2O ($Os(bpy)_3^{2+}$) and acetonitrile ($Os(bpy)_3^{2+}$, $Os(bpy)_2(P_2)^{2+}$, and $Os(bpy)(P_2)_2^{2+}$). The concentration of complexes for the Raman study was approximately 10^{-4} M in all cases.

Results

Emission Spectra and Spectral Fits. Low-temperature (77 K) emission spectra are shown in Figure 1 along with spectral fits of the data. Note the development of the equations used in the Appendix. The calculated spectra were obtained by using the parameters in Table I and eq 1 and 2. As is characteristic of other Ru(II) and Os(II) polypyridine complexes, vibrational progressions in the range 1200–1400 cm^{-1} appear in the emission spectra.[5] The resolved vibrational components have frequency spacings typical of ν(bpy) ring stretching vibrations.[9,16]

Using the spectral fitting procedure described previously[13] (and in the Appendix) we have determined the structural parameters S_M and S_L for high- and low-frequency vibrational components in the spectra. The values obtained in the fits are summarized in Table I. Although no distinct progression due to the low-frequency (400 cm^{-1}) modes appears in the spectra, the quality of the spectral fits, i.e., the apparent bandwidth of the vibrational components for $v_M > 0$, relies on their inclusion. In an earlier study it was shown that for a series of related complexes of Os(II) there are internally consistent, systematic variations in S_L with changes in ligands.[13a,17] That work will be discussed in a

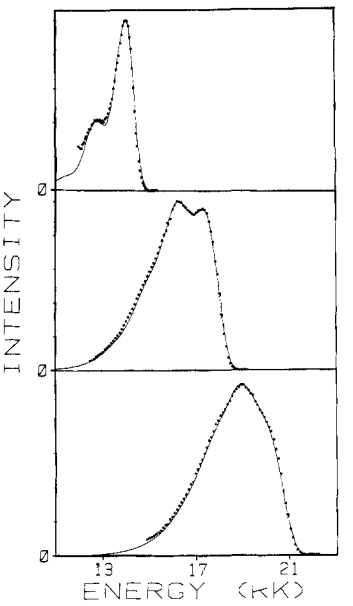

Figure 1. Corrected emission spectra of $Os(bpy)_3^{2+}$ (top), $Os(bpy)_2(P_2)^{2+}$ (middle), and $Os(bpy)(P_2)_2^{2+}$ (bottom). Conditions: 77 K, 4:1 ethanol/methanol glass, PF_6^- salts. The points represent the experimental spectra; the solid lines are the calculated spectra using the parameters given in Table I (see text). Emission intensities are given in arbitrary units.

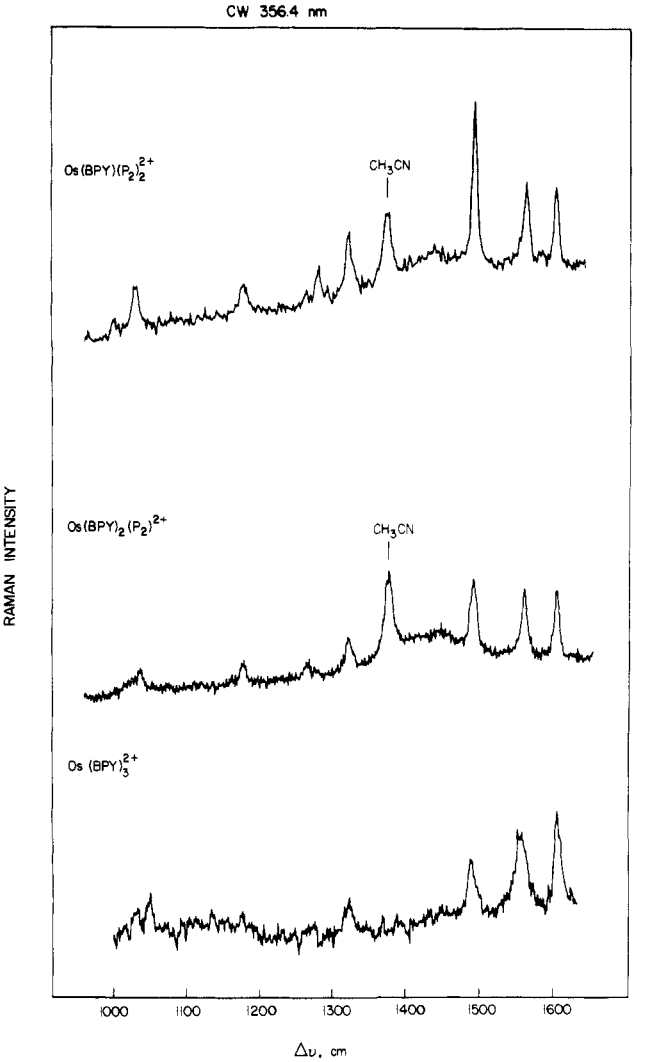

Figure 2. Ground-state resonance Raman spectra of the osmium complexes studied, obtained by using the 356.4-nm line of the CW Kr^+ laser (power ca. 100 mW at the sample).

(14) (a) McCoy, E. F.; Ross, I. G. *Aust. J. Chem.* **1962**, *15*, 573. (b) Ballhausen, C. J. "Molecular Electronic Structure of Transition Metal Complexes"; McGraw-Hill: New York, 1979.
(15) Parker, C. A.; Rees, W. T. *Analyst* **1960**, *85*, 587.
(16) (a) Clark, R. J. H.; Turtle, P. C.; Strommen, D. P.; Streusand, B.; Kincaid, J.; Nakamito, K. *Inorg. Chem.* **1977**, *16*, 84. (b) Kincaid, J., personal communication, 1983.

Table I. Emission Spectral Fitting Parameters[a]

complex	$\bar{\nu}_{00}$, cm^{-1}	S_M	S_L	$\bar{\nu}_M$, cm^{-1}	$\bar{\nu}_L$, cm^{-1}	$\bar{\nu}_{1/2}$, cm^{-1}
$Os(bpy)_3^{2+}$	14 175 ± 23	0.53 ± 0.02	0.87 ± 0.08	1325 ± 20	400 ± 10	635 ± 44
$Os(bpy)_2(P_2)^{2+}$ [b]	18 000 ± 61	1.15 ± 0.02	2.20 ± 0.20	1350 ± 20	400 ± 7	650 ± 113
$Os(bpy)(P_2)_2^{2+}$ [b]	20 900 ± 152	1.31 ± 0.02	3.00 ± 0.53	1325 ± 21	400 ± 16	675 ± 331
$Ru(bpy)_3^{2+}$	17 390 ± 50	1.00 ± 0.03	1.20 ± 0.18	1380 ± 22	400 ± 12	625 ± 95
$Ru(bpy)_2(en)^{2+}$ [c]	14 900 ± 61	0.86 ± 0.05	0.9 ± 0.22	1350 ± 35	400 ± 25	700 ± 116
$Re(bpy)(CO)_3Cl$	19 925 ± 236	1.30 ± 0.03	2.4 ± 0.59	1450 ± 42	500 ± 28	775 ± 416

[a] Note eq 1 and 2 and the calculated spectra using these values in Figure 1. The parameters are defined in the Experimental Section. [b] P_2 is *cis*-$Ph_2PCH{=}CHPPh_2$. [c] en is ethylenediamine.

Table II. Resonance Raman Frequencies as Wavenumbers (cm^{-1}) for the Ground and MLCT Excited States of Osmium(II) Bipyridine Complexes and for Bipyridine Radical Anion

$Os(bpy)_3^{2+}$			$Os(bpy)_2(P_2)^{2+}$			$Os(bpy)(P_2)_2^{2+}$			$Li^+(bpy^{-}\cdot)$	
ground state	MLCT state	δ_{vib}[a]	ground state	MLCT state	δ_{vib}[a]	ground state	MLCT state	δ_{vib}[a]	$\nu(bpy^{-}\cdot)$	δ_{vib}[d]
	749			742			743		752	
1029	1023		1018	1015		1005	1011		992	
1048	1045		1034	1036		1032	1031		1019	
	1107			1097			1101			
1175	1176		1178	1177		1180	1180			
	1220*	48		1214*	55		1209*	59	1206	62
1268*			1269*			1268*				
						1284				
						1294				
	1288*	34		1280*	43		1280*	46	1243	49
1322*	1325		1323*	1324		1326*	1325			
	1429*	62		1427*	65		1422*	76	1407	84
				1481[b]			1481[b]			
1491*	1496		1492*	1494		1498*	1500[c]			
	1512*	46		1509*	55		1500[c]	67	1486	72
1558*	1558[c]	52	1564*			1567*				
	1558*[c]			1552*	57		1545*	64	1554	56
1610*	1610		1609*	1605*		1609*	1609			

[a] $\delta_{vib} = \bar{\nu}$(ground state) − $\bar{\nu}$(MLCT state) for the asterisked frequency pairs. See text. Mode correlations (for $Os(bpy)_3^{2+}$) used to calculate δ_{vib} are as follows (MLCT state, ground state): 1220, 1268; 1288, 1322; 1429, 1491; 1512, 1558; 1558, 1610 cm^{-1}. [b] The 1481-cm^{-1} peak is the first overtone of the 742–743-cm^{-1} peak. This overtone is obscured in $Os(bpy)_3^{2+}$ by the 1496-cm^{-1} fundamental. [c] Accidentally degenerate neutral bpy and $bpy^{-}\cdot$ frequencies. [d] From $Os(bpy)_3^{2+}$ ground state.

forthcoming paper. It is worth noting here that in the fits, the derived values of $\bar{\nu}_M$ and S_M are relatively insensitive to $\bar{\nu}_L$ and S_L.

Resonance Raman and Time-Resolved Resonance Raman Spectroscopy. Resonance Raman (RR) spectra of the ground electronic states of the series $Os(bpy)_3^{2+}$, $Os(bpy)_2(P_2)^{2+}$, and $Os(bpy)(P_2)_2^{2+}$ were obtained by CW laser excitation using the 356.4-nm line of the Kr^+ laser. The ground-state RR spectra are shown in Figure 2. For all three complexes, this excitation wavelength provides considerable RR enhancement due to the bpy $\pi \rightarrow \pi^*$ transition at approximately 285 nm. Accordingly, the bpy modes that experience greatest enhancement are the seven symmetric in-plane C–C and C–N stretches which are typically observed in charge-transfer or $\pi \rightarrow \pi^*$ RR spectra of bpy complexes.[9,16] These seven stretches are, to a good approximation, represented by the seven most prominent peaks observed in the spectra in Figure 2. The spectra of $Os(bpy)_2(P_2)^{2+}$ and $Os(bpy)(P_2)_2^{2+}$ contain an additional peak at 1375 cm^{-1}, which is due to the CH_3 deformation mode of the CH_3CN solvent. No prominent peaks due to the diphosphine ligands are observed in the spectra of either $Os(bpy)_2(P_2)^{2+}$ or $Os(bpy)(P_2)_2^{2+}$, although weak features near 1280 cm^{-1} may be assignable to non-bpy modes.

The ground-state RR spectra exhibit a systematic variation in relative peak intensity, especially of the three peaks in the 1500–1600-cm^{-1} range, through the series of complexes studied. For $Os(bpy)_3^{2+}$, for which the MLCT transition is at much longer wavelength than the ca. 350-nm laser line, the primary resonance effect is due to the bpy $\pi \rightarrow \pi^*$ transition at ca. 300 nm. We ascribe the variation in relative intensity to increasing contribution to RR enhancement by the low-lying MLCT electronic transitions, which move to successively higher energy and therefore closer to the laser wavelength with increasing $d\pi-\pi^*$ energy gap through the series $Os(bpy)_3^{2+} \rightarrow Os(bpy)(P_2)_2^{2+}$.

The time-resolved resonance Raman spectra of the MLCT states of the three Os complexes are shown in Figure 3. Essentially complete (≥90%) saturation of the excited state was achieved for the $Os(bpy)_2(P_2)^{2+}$ and $Os(bpy)(P_2)_2^{2+}$ complexes, which have lifetimes of 500 and 1680 ns, respectively, in acetonitrile at room temperature.[13a] This fact was confirmed by observation of luminescence intensity as a function of laser pulse energy. In the case of $Os(bpy)_3^{2+}$, which has an excited-state lifetime of only 20 ns, approximately 60% saturation was achieved. Therefore, the time-resolved resonance Raman spectra of the mixed complexes are almost entirely due to the MLCT state, while the time-resolved resonance Raman spectrum of $Os(bpy)_3^{2+}$ has a minor but significant contribution from the ground state.

The RR frequencies of the ground and MLCT excited states of the complexes are summarized in Table II. This table also presents the parameter δ_{vib}, the difference in frequency between the radical-like bpy ligand in the MLCT state and the neutral bpy ligands in the ground electronic state. The δ_{vib} values are given only for the five prominent modes above 1200 cm^{-1}, because they apparently contain the greatest contribution from C–C and C–N stretches[16b] and because mode correlations between neutral bpy and bpy radical are most reliable for these five peaks.

Discussion

The complexes $Os(bpy)_3^{2+}$, $Os(bpy)_2(P_2)^{2+}$, and $Os(bpy)(P_2)_2^{2+}$ constitute a set in which (1) the nature of the lowest excited states, $d\pi(Os) \rightarrow \pi^*(bpy)$ MLCT, has the same orbital origin throughout the series, (2) the energy of the excited state above the ground state as evidenced by emission spectra (see Table I) varies systematically, (3) the complexes are thermally and photochemically inert, (4) quantum yields for emission are sufficiently high for reliable measurements to be made of emission spectra and ex-

(17) Caspar, J. V.; Meyer, T. J., manuscript in preparation.

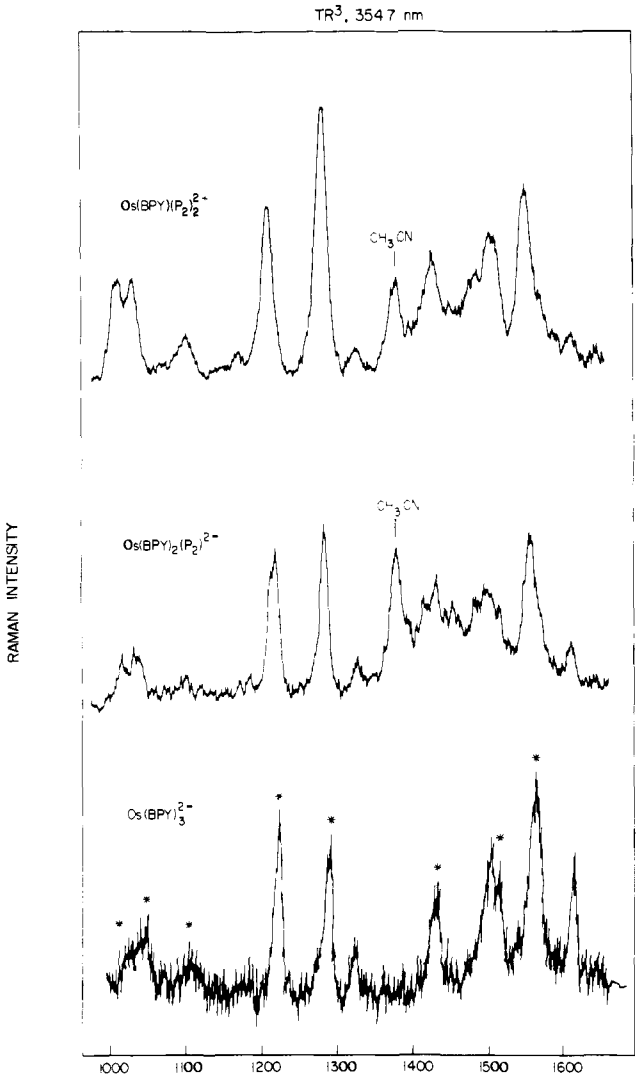

Figure 3. Time-resolved resonance Raman spectra of the MLCT states of the osmium complexes studied, obtained by using the third harmonic (354.7 nm) of the pulsed Nd:YAG laser (per-pulse energy ca. 3 mJ).

cited-state lifetimes, and (5) optical properties, e.g., lifetime and absorption spectra, are suitable for examination of the excited-state resonance Raman spectra by straightforward time-resolved resonance Raman techniques.

The series of related complexes therefore represents an opportunity to explore some fundamental issues in the photophysics of MLCT excited states. For example, using a more extended series of complexes it has proven possible to demonstrate the validity of the energy gap law for radiationless decay.[13a,18] The issues of interest in this study are, first, the question of localization or delocalization of the excited electron in complexes like Os(bpy)$_3^{2+}$ where there are multiple chromophoric ligands. Secondly, given the existence of ground- and excited-state Raman data and of Franck–Condon analyses from low-temperature emission spectral fits, there seems a clear possibility of obtaining detailed insight into variations in excited-state structure through the series.

Localization vs. Delocalization. Our previous time-resolved resonance Raman studies of M(bpy)$_3^{2+}$ complexes (M = Ru, Os)[9] and related work from other laboratories[10,11] have examined the question of whether the MLCT excited states of these and related complexes should be considered as being "delocalized", i.e., represented as $M^{III}(bpy^{-1/3})_3^{2+}$ as had been suggested by earlier photophysical studies, or "localized", i.e., represented as $M^{III}(bpy)_2(bpy^{-}\cdot)^{2+}$. The localized formulation was demonstrated for Ru(bpy)$_3^{2+}$ by several criteria[9-11] and was strongly suggested[9b] for Os(bpy)$_3^{2+}$ by comparison of the excited-state bpy frequencies to those of bpy$^{-}\cdot$ produced by chemical reduction. Because of the short lifetime of the emitting MLCT state for Os(bpy)$_3^{2+}$ it was not possible in the earlier work to obtain definitive time-resolved resonance Raman evidence that the MLCT state(s) for Os(bpy)$_3^{2+}$ are localized.

The present study offers an opportunity to test unambiguously the localized hypothesis for the Os complexes. If the lowest excited state is $d\pi(Os) \rightarrow \pi^*(bpy)$ MLCT in each case, the localized and delocalized hypotheses predict quite different results for the excited-state Raman frequencies of the bpy modes. If the delocalized case were correct, the MLCT states of the complexes are represented as $Os^{III}(bpy^{-1/3})_3^{2+}$, $Os^{III}(bpy^{-1/2})_2(P_2)^{2+}$, and $Os^{III}(bpy^{-})(P_2)_2^{2+}$. If the localized case were valid, the electronic distribution is represented as $Os^{III}(bpy)_2(bpy^{-}\cdot)^{2+}$, $Os^{III}(bpy)(bpy^{-}\cdot)(P_2)^{2+}$, and $Os^{III}(bpy^{-}\cdot)(P_2)_2^{2+}$ for the three different complexes. The delocalized hypothesis predicts a single set of bpy C–C and C–N stretches for the MLCT state of each complex in the series, with frequencies that range from slightly lower than the ground state (for $bpy^{-1/3}$ in Os(bpy)$_3^{2+}$) to nearly those of bpy$^{-}\cdot$ (for bpy^{-} in Os(bpy)(P$_2$)$_2^{2+}$). On the other hand, the localized hypothesis predicts that all three complexes in the MLCT state will exhibit a set of bpy frequencies near those of bpy$^{-}\cdot$ and in addition that Os(bpy)$_3^{2+}$ and Os(bpy)$_2$(P$_2$)$^{2+}$ will possess a set of bpy modes characteristic of neutral bpy. Under ideally saturated conditions, the "neutral bpy" modes will be absent in the MLCT state of Os(bpy)(P$_2$)$_2^{2+}$.

Table II and Figures 2 and 3 clearly show that the localized hypothesis is correct. Each complex in its MLCT state exhibits a set of bpy frequencies that are shifted from their ground-state values by amounts (δ_{vib}, Table II) approximately those observed for bpy$^{-}\cdot$. Small but significant differences exist among these "bpy$^{-}\cdot$" frequency shifts, and these differences will be discussed in detail below. An additional observation in support of the localized hypothesis is that the "neutral bpy" peaks virtually disappear in the time-resolved resonance Raman spectrum of Os(bpy)(P$_2$)$_2^{2+}$ (compare relative intensities for the 1609-cm^{-1} peaks in the three time-resolved resonance Raman spectra). Given the fact that localization has been shown to be the appropriate description in the cases cited earlier, in Ru(bpy)$_2$(en)$^{2+}$[9b] and, more recently, in Re(bpy)(CO)$_3$Cl,[11] it seems reasonable to conclude that localization of the excited electron on the vibrational time scale in MLCT excited states of this kind is a common feature.

Variations in the "Energy Gap". It is clear from the emission maxima given in Table I that the effect of substituting phosphine ligands for bpy is to increase the energy gap between the MLCT excited state and the ground state. Both the absorption and emission energies vary in the order Os(bpy)$_3^{2+}$ < Os(bpy)$_2$(P$_2$)$^{2+}$ < Os(bpy)(P$_2$)$_2^{2+}$. The origin of such effects appears to be twofold: (1) stabilization of the ground state by enhanced $d\pi(Os)$–$d\pi(P)$ back-bonding, compared to $d\pi(Os)$–$\pi^*(bpy)$ back-bonding, and (2) destabilization of the excited state by loss of σ-electron donation to Os(III) as bipyridyl ligands are replaced by phosphines. It is known from electrochemical measurements[13a,20,21] that variations in the relative π^* energies of the bpy ligands as the remaining ligands are varied are relatively small.

If changes in $d\pi$–π^* back-bonding between Os and bpy in the ground state were significant as the P$_2$ ligands are substituted for bpy, noticeable shifts would be expected to occur in ground-state bpy Raman frequencies. Examination of the ground-state fre-

(18) (a) Caspar, J. V.; Sullivan, B. P.; Kober, E. M.; Meyer, T. J. *Chem. Phys. Lett.* **1982**, *91*, 91. (b) Caspar, J. V.; Kober, E. M.; Sullivan, B. P.; Meyer, T. J. *J. Am. Chem. Soc.* **1982**, *104*, 630. (c) Caspar, J. V.; Meyer, T. J. *J. Phys. Chem.* **1983**, *87*, 952. (d) Caspar, J. V.; Meyer, T. J. *Inorg. Chem.* **1983**, *22*, 2444. (e) Caspar, J. V.; Meyer, T. J. *J. Am. Chem. Soc.* **1983**, *105*, 5583.

(19) (a) Strukl, J. S.; Walter, J. L. *Spectrochim. Acta, Part A* **1971**, *27A*, 209. (b) *Ibid.* **1971**, *27A*, 223.

(20) (a) Sullivan, B. P.; Salmon, D. J.; Meyer, T. J. *Inorg. Chem.* **1978**, *17*, 3334. (b) Dressick, W. J.; Marshall, J. W.; Sullivan, B. P.; Caspar, J. V.; Kober, E. M.; Meyer, T. J., manuscript in preparation.

(21) Miskowski, M. H.; Gray, H. B.; Woodruff, W. H. *J. B. S. Lett.* **1981**, *69*, 175.

quencies in the 1000–1700-cm^{-1} range (Table II) shows that the two lowest frequency modes decrease in frequency upon substitution by P_2 while the higher frequency modes are shifted to higher frequency or remain unchanged. The pattern of shifts suggest that the distribution of π-electron density within the bpy ligands is indeed different between $Os(bpy)_3^{2+}$ and the mixed-chelate complexes. However, the *net* frequency shifts of $\sim$−2 cm^{-1} per Raman mode clearly imply that only small changes in net bpy π-electron density exist among these complexes. It has been estimated that the extent of $d\pi$–π^*(bpy) mixing in complexes of this type may be in the range 10–20%.[22] However, variations in the π^*(bpy) levels with changes in the remaining ligands are usually expected to be small because interactions between the ligands are indirect in that they arise from variations in metal–ligand mixing induced by another ligand. These conclusions are consistent with a large body of information[9,16,23,24] on bipyridine complexes, which suggests that, with isolated exceptions such as $Ru^{II}(NO)$, Mo(II), and Os(IV) complexes, where the electronic characteristics of the metal are unusually electron rich or electron deficient,[25-27] net π-electron density at the bpy ligand is independent of the changes in π donor–acceptor characteristics of the metal, at least in a gross way.

In the MLCT excited states, however, substantial $d\pi$(Os)–π^*(bpy) interactions are suggested by the shifts observed in the Raman frequencies in the series $Os(bpy)_3^{2+}$–$Os(bpy)_2(P_2)^{2+}$–$Os(bpy)(P_2)_2^{2+}$. In our earlier work[9b] on the MLCT states of $M(bpy)_3^{2+}$, it was noted that the Raman frequencies for the radical-like bpy ligand were higher for M = Os than for M = Ru. The suggestion was made there that this was a consequence of greater $d\pi$(Os(III)) mixing, with the π^*(bpy) orbital formally occupied by the excited electron. More extensive mixing is expected for Os compared to Ru because of a greater $d\pi$ radical extension and because the $d\pi$ levels for Os(III) are closer in energy to the excited electron in π^*(bpy) as shown both by electrochemical measurements[20] and by the fact that the emission energy is lower for M = Os. According to this analysis, the ligand-based orbital in the MLCT transition possesses more metal character for M = Os than for M = Ru. It follows that in the excited state the "bpy$^-$·" ligand is less radical-like for M = Os, contains less transferred π^*-electron density, and therefore has higher vibrational frequencies.

If the energy gap between ground and excited states, as evidenced by the emission energy, is a factor in determining the apparent extent of charge transfer, the series of complexes of interest here provides a useful basis for for exploring the point in further detail. In the three complexes the same metal is involved, but significant differences in emission energies exist. As the excited-state–ground-state energy gap increases, the extent of $d\pi$(Os(III))–π^*(bpy) mixing is expected to diminish, the extent of charge transfer to bpy in the MLCT state should increase, and the acceptor redox orbital should become more purely π^*(bpy) in character. This predicted behavior is clearly borne out by the δ_{vib} values in Table II, which systematically approach those of bpy$^-$· in the order $Os(bpy)_3^{2+} < Os(bpy)_2(P_2)^{2+} < Os(bpy)(P_2)_2^{2+} < Li^+(bpy^-\cdot)$, which is also the order of increasing emission energy for the three complexes.

The same behavior, but with its origin in a different observation, has been reported for related complexes of 1,10-phenanthroline (phen) for a series of complexes of the type $(phen)OsL_4^{2+}$ (L = py, $^1/_2$ bpy, PR_3, ...). For the series of complexes, it has been shown from spectral fits of vibrational structure at 77 K[13a] that systematic variations in the extent of phen distortion in the excited state occur with an increase in emission energy.

Table III. Extent of Metal-to-Ligand Charge Transfer (x) in the MLCT Excited States for Osmium(II), Ruthenium(II), and Rhenium(I) Complexes[a]

$$[M^n(bpy)^0] \xrightarrow{MLCT} [M^{n+x}(bpy)^{x-}]$$

complex	$\bar{\delta}_{vib}^-$ (G-E),[b] cm^{-1}	$\bar{\delta}_{vib}^-$ (bpy^0–$bpy^-\cdot$),[c] cm^{-1}	x
$Os(bpy)_3^{2+}$	48	65	0.74
$Os(bpy)_2(P_2)^{2+}$	55	66	0.83
$Os(bpy(P_2)_2^{2+}$	62	68	0.91
$Ru(bpy)_3^{2+}$	54	65	0.83
$Ru(bpy)_2(en)^{2+}$	52	66	0.79
$Re(bpy)(CO)_3Cl$	53	63	0.84

[a] See text and eq 3 for a discussion of the determination of x. [b] Average difference in frequency between complexed bpy stretching modes in the ground and MLCT states. [c] Average change in frequency between complexed bpy modes in the ground state (bpy^0) and those in $Li^+(bpy^-\cdot)$.

Extent of Charge Transfer. It has been shown that, in organic π-radical systems, the frequency of a given normal mode is linearly related to the charge on the radical.[28-30] The point was demonstrated based on the series $TCNQ^0$, $TCNQ^-$, $TCNQ^{2-}$ (TCNQ = tetracyanoquinodimethane) and a series of partially reduced $TCNQ^{x-}$ species, where the fractional charge x was defined by the solid-state stoichiometry. If such a relationship were valid for the "bpy$^-$·" in the MLCT excited state case of interest here, the extent of charge transfer from the metal to the ligand in the MLCT state can be calculated trivially based on (1) ground-state "bpy^0" frequencies, (2) excited-state "bpy$^-$·" frequencies, and (3) frequencies for bpy$^-$· as in $Li^+(bpy^-\cdot)$. The requisite frequencies are given in Table II, and the δ_{vib} values were used to calculate the quantity x in eq 3, where x is the fractional charge of the radical-like bipyridine ligand in the MLCT state. The values

$$x = \frac{\delta_{vib}(\text{ground} \rightarrow \text{MLCT})}{\delta_{vib}(\text{ground} \rightarrow bpy^-\cdot)} \quad (3)$$

of x for the osmium complexes are given in Table III. These are average x values obtained by using the five highest frequency Raman modes as discussed above. The charge-transfer data for $Ru(bpy)_3^{2+}$, $Ru(bpy)_2(en)^{2+}$, and $Re(bpy)(CO)_3Cl$ are included for comparison.[9,11] For a given metal, the values of x vary as expected with the energy gap between ground and excited states as taken by the emission energies.

Excited-State Structure from Vibrational Data. The observation that frequencies of correlated vibrational modes between ground and electronically excited states vary systematically offers, in principle, the opportunity to determine equilibrium bond length displacements between the two states. For similar bonding situations, the force constants of chemical bonds are related to bond length based on the well-known Badger rule[31] and more recent refinements of the same basic idea.[32] In the present system, we can (1) unambiguously identify bipyridine ligand vibrations by their frequencies, (2) determine the symmetries of the vibrations by depolarization ratio measurements, and (3) infer which are predominantly C–C and C–N stretches by the magnitude of their resonance enhancement with MLCT or bpy-centered $\pi \rightarrow \pi^*$ electronic transitions and by deuterium shifts. The procedure involved for both ground and excited states has been the subject of several studies.[9,16,33,34] Having identified the symmetric C–C

(22) Kober, E. M. Ph.D. Thesis, The University of North Carolina, Chapel Hill, NC, 1982.
(23) Asano, M.; Koningstein, J. A.; Nicollin, D. *J. Chem. Phys.* **1980**, *73*, 688.
(24) (a) Nakamoto, K. "Infrared and Raman Spectroscopy of Infrared and Coordination Compounds", 3rd ed.; Wiley: New York, 1977. (b) Konig, E.; Lindner, E. *Spectrochim. Acta Part A* **1972**, *28A*, 1393.
(25) Callahan, R. W.; Meyer, T. J. *Inorg. Chem.* **1977**, *16*, 574.
(26) Guadiello, J. G.; Bradley, P. G.; Norton, K. A.; Woodruff, W. H.; Bard, A. J. *J. Am. Chem. Soc.*, submitted.
(27) Chisholm, M. H.; Hoffman, J. C.; Rothwell, I. P.; Bradley, P. G.; Kress, N.; Woodruff, W. H. *J. Am. Chem. Soc.* **1981**, *103*, 4945.
(28) Van Duyne, R. P.; Suchanski, M. R.; Lakovits, J. M.; Siedle, A. R.; Parks, K. D.; Cotton, T. M. *J. Am. Chem. Soc.* **1979**, *101*, 2832.
(29) Suchanski, M. R. Ph.D. Thesis, Northwestern University, 1978.
(30) Cape, T. C. Ph.D. Thesis, Northwestern University, 1978.
(31) Badger, R. M. *J. Chem. Phys.* **1934**, *2*, 128; **1935**, *3*, 710; *Phys. Rev.* **1935**, *48*, 284.
(32) Herschbach, D. R.; Laurie, V. W. *J. Chem. Phys.* **1961**, *35*, 458.

Table IV. Average Bond Distance Displacements $\Delta\bar{r}$ for Bipyridine between the Ground and MLCT States for $Os(bpy)_n(P_2)_{3-n}^{2+}$

complex	$\Delta\bar{r}_{em}$,[a] Å	$\Delta\bar{r}_{vib}$ (Å) for indicated $\bar{\upsilon}_{Raman}$ (cm^{-1})[b]				
		1268	1322	1491	1558	1610
$Os(bpy)_3^{2+}$	0.0126 ± 0.0005	0.0158	0.0106	0.0173	0.0122	0.0134
$Os(bpy)_2(P_2)^{2+}$	0.0184 ± 0.0004	0.0181	0.0135	0.0182	0.0146	0.0147
$Os(bpy)(P_2)_2^{2+}$	0.0199 ± 0.0004	0.0194	0.0144	0.0213	0.0178	0.0166

[a] Calculated from S_M values in Table I using eq 7. [b] $\Delta\bar{r}_{Raman}$ calculated by Badger's rule as described in the text from RR mode frequency pairs correlated between the ground state and MLCT state of each complex. Values of $\bar{\upsilon}_{Raman}$ refer to $Os(bpy)_3^{2+}$ (ground state).

and C–N stretches with the seven most intense resonance Raman modes in the 1000–1700-cm^{-1} region, and most reliably with the five modes above 1200 cm^{-1}, we can in principle employ Badger's rule to calculate Δr, the bond length displacement between the ground-state bond lengths (r_e) and those of the MLCT state (r_e^*) according to eq 4.[32] Here, ν_{vib} and ν^*_{vib} are the vibrational

$$\Delta r = r_e^* - r_e = \ln(\nu_{vib}/\nu^*_{vib})/2.45 \quad (4)$$

frequencies in the ground and MLCT states, respectively, and 2.45 is an empirical constant that scales the Badger rule relationship for C–C and C–N bonding.[32]

In practice, Badger's rule has several possible difficulties in its application to the present systems. It is not clear whether the rule, which was intended to evaluate ground-state structural changes, is applicable to molecules in different electronic states. In the present case, on the other hand, which essentially compares an organic molecule with its π radical anion, there are no fundamental changes in bonding involved. It is interesting to note that Badger's rule has been shown to be applicable to neutral organics and their π-anion radicals.[28,35] A second difficulty is that there is no guarantee that even if the rule is applicable to the present system, the empirical constant in eq 4 (which was determined for diatomics and other simple molecules) is valid for 2,2′-bipyridine and other complex molecules. However, application of eq 4 to the $TCNQ^{0,-,2-}$ system[35] reproduces the independently determined bond distance displacements satisfactorily. A final difficulty is that the observed Raman frequencies involve complex normal modes in which many local coordinate displacements are obligatorily coupled and are not, at least in general, localized vibrations of a particular bond. This does not invalidate Badger's rule, but it means that a Δr value calculated by eq 4 for a vibrational mode of bipyridine will not correspond to a specific bond displacement. Rather, such a Δr value represents a weighted average of the displacements of all the bonds whose stretching motions contribute to the potential energy distribution (PED) of the normal mode in question.[35,36] We shall denote this quantity $\Delta\bar{r}_{vib}$, the PED-weighted average bond displacement, the value of which will generally be dependent upon the identity of the vibrational mode selected. In such a case, Δr values of specific bonds can be determined if sufficient vibrational data are known and reliable PED's have been determined by vibrational analysis. However, the fundamental question remains as to the applicability and reliability of Badger's rule in the present case.

Excited-State Structure from Franck–Condon Analysis. Fortunately, an independent approach to determination of excited-state structure is available based on a Franck–Condon analysis of vibrational progressions observed in absorption or emission spectra.[13a,14] Since the time-resolved resonance Raman experiment samples the principle excited state present $\gtrsim$1 ns after excitation, the time-resolved resonance Raman spectra involve the same excited state, viz., the "triplet charge-transfer" state(s) rather than the "single charge-transfer" transitions that dominate absorption.[5,6,8] The spectral fitting procedure involved is described above and in the Appendix.

The relevant experimental parameters obtainable from the spectral fitting procedure are S_M and S_L. These parameters are related to the extent of excited-state distortion in the medium-frequency ν(bpy) and low-frequency ν(metal–N or metal–P) deactivating vibrations, respectively. There are at least seven Raman-active modes in the frequency range of interest (Table II), any or all of which may be Franck–Condon active in emission. Therefore, S_M derived from the spectral fitting procedure may well be an averaged quantity reflecting contributions from several ν(bpy) modes. As noted above, although no resolved vibrational progression for the ν(M–L) modes is observed in the emission spectra, their inclusion in eq 1 is required to reproduce satisfactorily the bandwidths of the higher energy components. Because of the low frequencies involved, the ν(M–L) modes make a relatively small contribution to excited-state decay; moreover, the value of S_M extracted from the spectral fits is relatively insensitive to the value of $\bar{\nu}$(M–L) chosen or to the magnitude of S_L.

S_M is related to the individual equilibrium bond distance changes between excited and ground states, $r_e^* - r_e$, defined above in the discussion involving Badger's rule, as shown in eq 5 and 6. In

$$S_M = (2\pi^2 M_M \nu_M/h)R^2 \quad (5)$$

$$S_M = \tfrac{1}{2}(\Delta_M)^2; \qquad \Delta_M = (M_M\omega_M/\hbar)^{1/2}R \quad (5a)$$

$$R = [\sum_{j=1}^{b}(r_e^* - r_e)_j^2]^{1/2} \quad (6)$$

eq 5 and 6, $\nu_M = c\bar{\nu}_M$ (c is the velocity of light in a vacuum) is the frequency of the "acceptor" mode, and the summation is taken over the 13 (b = 13 in eq 6) C–C and C–N bonds of the ligands. In eq 5a, eq 5 is written in terms of the dimensionless fractional coordinate Δ_M and $\omega_M = 2\pi\nu_M$ is the angular frequency of the vibration. The reduced mass, M_M, is taken to be 13, an appropriate value for a symmetric, in-phase aromatic ring breathing mode. Such a motion should effectively mimic the distortions involved between the "bpy^0" and "$bpy^{-\cdot}$" structures. It is not possible to extract individual bond displacements from eq 5 and 6, but rather S_M is related to the sum of the *absolute* bond displacements. From S_M we can extract the *average bond displacement*, $\Delta\bar{r}_{em}$, by rearranging eq 5 and 6 to give eq 7 (b = 13).

$$\Delta\bar{r}_{em} = \left(\frac{hS_M}{2\pi^2 M_M \nu_M b}\right)^{1/2} = \left(\frac{M_M\omega_M}{\hbar}\right)^{-1/2}\frac{\Delta_M}{b^{1/2}} \quad (7)$$

As noted above, the available evidence from ground-state resonance Raman experiments suggests that seven ligand-localized vibrations are resonantly enhanced by the MLCT transition and may therefore contribute to the observed emission spectra. Further evidence on this point comes from the spectral fitting results in Table I, where the best-fit value for the spacings in the vibrational progressions varies between 1325 and 1450 cm^{-1}, depending upon the complex, and similar variations have been observed for other, related series of excited states.[13a] If a single deactivating vibration were operative, the vibrational spacings in the fits should stay relatively constant. That they do not suggests that more than one mode is operative and their relative contributions may vary from complex to complex, perhaps varying with the energy gap. If this is the case, the vibrational spacings observed in the spectra and obtained in the fits are an average of several contributions. As

(33) Woodruff, W. H. *ACS Symp. Ser.* **1983**, *No. 211*, 473.
(34) Woodruff, W. H.; Dallinger, R. F.; Hoffman, M. Z.; Bradley, P. G.; Presser, D.; Malueg, V.; Kessler, R. J.; Norton, K. A. In "Proceedings of the 1st International Converence on Time-Resolved Vibrational Spectroscopy"; Atkinson, G. H., Ed.; Wiley: New York, in press.
(35) Jeanmaire, D. C.; Van Duyne, R. P. *J. Am. Chem. Soc.* **1976**, *98*, 4029.
(36) Wilson, E. B.; Decius, J. L.; Cross, P. C. "Molecular Vibrations"; Dover: New York, 1955.

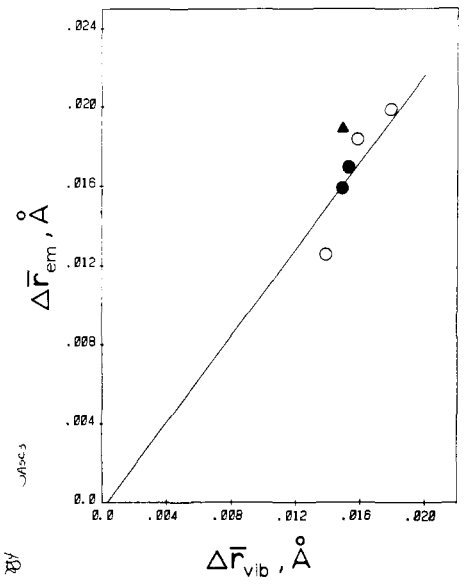

Figure 4. Plot of average bond length displacement of the bpy ligand in the MLCT state determined from emission data ($\Delta\bar{r}_{em}$) vs. that determined from Raman data ($\Delta\bar{r}_{vib}$). Open circles represent the osmium complexes studied, with the value of n (n = 0, 1, 2) in $Os(bpy)_n(P_2)_{3-n}^{2+}$ increasing from n = 0 to n = 2 as shown. Filled circles represent the ruthenium complexes: upper, $Ru(bpy)_3^{2+}$; lower, $Ru(bpy)_2(en)^{2+}$. The filled triangle represents *fac*-$Re(bpy)(CO)_3Cl$. The slope is 1.1.

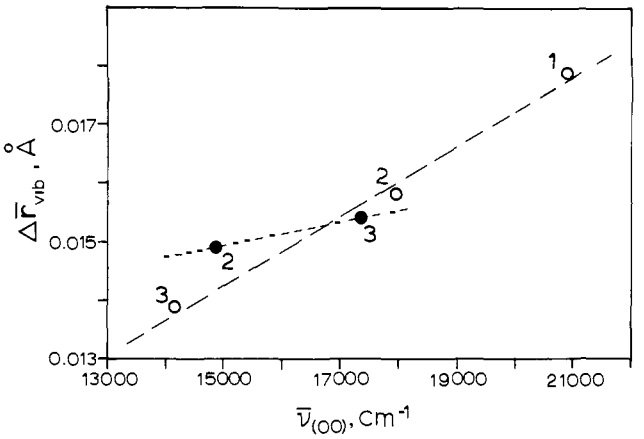

Figure 5. Plot of average bond length displacement of the bpy ligand in the MLCT state determined from Raman data ($\Delta\bar{r}_{vib}$) vs. emission energy (0–0 transition) for the Os and Ru complexes. Open circles, osmium points: (3) $Os(bpy)_3^{2+}$; (2) $Os(bpy)_2(P_2)^{2+}$; (1) $Os(bpy)(P_2)_2^{2+}$. Filled circles, ruthenium points: (3) $Ru(bpy)_3^{2+}$; (2) $Ru(bpy)_2(en)^{2+}$.

a consequence, use of the single-mode spectral fitting procedure to obtain $\Delta\bar{r}_{em}$ values from eq 7 has the effect of averaging contributions from the various normal modes. When added together these individual contributions would lead to the experimentally observed values for S_M.[37]

Comparison of Results

The results of the Badger rule calculations from the time-resolved resonance Raman data and of the emission bandshape analyses are compared in Table IV. Values of $\Delta\bar{r}_{vib}$ are included for each of the five modes above 1200 cm^{-1}. It is not surprising that the $\Delta\bar{r}_{vib}$ values differ from one another, because each is weighted by the PED of the individual normal modes in question. A given normal mode may be dominated by internal coordinates which may have values of $r_e^* - r_e$ quite different from the average. If the $\Delta\bar{r}_{vib}$ values are realistic and reliable PED's can be determined for the ligand, simultaneous equations can be solved for the individual $r_e^* - r_e$ values for each bond. Therefore it is possible in principle to calculate the structure of the ligand in the MLCT excited state. However, the question remains as to the reliability of the $\Delta\bar{r}_{vib}$ values as estimated by the Badger rule procedure.

Table IV also gives the values of $\Delta\bar{r}_{em}$ calculated from S_M values using eq 7. If the $\Delta\bar{r}_{em}$ values for each complex are compared to the average value of $\Delta\bar{r}_{vib}$, agreement in each case is within experimental error: (1) for $Os(bpy)_3^{2+}$, $\Delta\bar{r}_{em}$ = 0.0126 ± 0.0005 Å, $\Delta\bar{r}_{vib}^{av}$ = 0.014 ± 0.003 Å; (2) for $Os(bpy)_2(P_2)^{2+}$, 0.0184 ± 0.0004, 0.016 ± 0.002; (3) for $Os(bpy)(P_2)_2^{2+}$, 0.0199 ± 0.0004, 0.018 ± 0.003.

Figure 4 shows a plot of $\Delta\bar{r}_{em}$ vs. $\Delta\bar{r}_{vib}$. The line is considered to pass through the origin because, if the average absolute value $\Delta\bar{r}_{em}$ is zero, each individual bond displacement must be zero and so must every $\Delta\bar{r}_{vib}$. The slope of the line through the origin and the points representing the three osmium complexes is 1.1. The experimental points for $Ru(bpy)_3^{2+}$, $Ru(bpy)_2(en)^{2+}$, and $Re(bpy)(CO)_3Cl$ are included for comparison. The results show that two entirely different approaches to the determination of excited-state bond displacements agree to within an average of one *thousandth*, and a maximum of three *thousandths*, of an angstrom unit, approximately the precision expected of a high-quality X-ray crystal structure. The agreement and the linear correlation of the points in Figure 4 are striking in view of the approximations involved in the detemination of $\Delta\bar{r}_{em}$ and $\Delta\bar{r}_{vib}$. The two approaches to the determination of $\Delta\bar{r}$ are entirely independent of one another. Indeed, the Franck–Condon analysis, which assumes only linear vibronic coupling, discounts the possibility of differing vibrational frequencies in the two electronic states. Badger's rule, on the other hand, fundamentally disregards the existence of any but the ground electronic state. We regard the agreement between the two approaches, which in fundamental ways are mutually exclusive, as a validation of the $\Delta\bar{r}$ values obtained by both approaches and also as further validation of the Herschbach–Laurie empirical constants[32] in their application to complex molecular systems.

At present, the $\Delta\bar{r}_{vib}$ values must be considered the more reliable of the two sources of structural information described here. We estimate that these average displacements are accurate to within a few thousandths of an angstrom. Their precision is ±0.001 Å, based on the precision of the Raman frequencies.

The trend in $\Delta\bar{r}$ in the three Os complexes studied, as reflected in the time-resolved resonance Raman results and in the emission bandshape analyses, is toward an increase in $\Delta\bar{r}$ with increasing ground- to excited-state energy gap. The trend is consistent with an increasing degree of reduction at the ligand as the emission energy increases. As noted before, in orbital terms this means that the acceptor orbital of the luminophores has an increasing degree of π^*(bpy) character and a decreasing degree of Os character as the energy gap increases. The same qualitative behavior is observed in the two Ru complexes in Figure 4, $Ru(bpy)_3^{2+}$ and $Ru(bpy)_2(en)^{2+}$. However, the quantitative relationship between $d\pi(M)-\pi^*(bpy)$ energy gap and $\Delta\bar{r}$ may be somewhat dependent on the metal component of the chromophore, which is to be expected given the differences in electronic structure involved. In Figure 5 is shown a plot of $\Delta\bar{r}$ vs. the 0–0 emission energy, $\bar{\nu}_{00}$, for the series of complexes. Perhaps with the acquisition of more data, it will be possible to establish a more quantitative, metal-dependent relationship between $\Delta\bar{r}$ and $\bar{\nu}_{00}$ and so gain further insight into the electronic structures of the excited states.

The results obtained here provide an important lead into the possible determination of the molecular structures of excited states in solution based on vibrational data. Our results suggest that if the ground-state structure is known and a reliable vibrational analysis is available for the complexed bipyridine ligand, precise structures for the ligand in the MLCT states under chemically relevant conditions (viz., in fluid solution) can be determined to accuracies within those accessible from X-ray crystallography. The same considerations apply to the low-frequency metal–ligand vibrations, although there the results of the curve-fitting procedure are probably not sufficiently well defined and direct observation by resonance Raman remains an experimental challenge. Nonetheless, it seems quite clear that a reasonably accurate de-

(37) Englman, R.; Jortner, J. *J. Mol. Phys.* **1970**, *18*, 145.

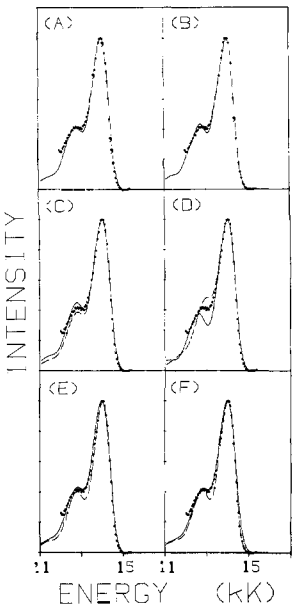

Figure 6. Dependence of calculated spectrum of $Os(bpy)_3^{2+}$ on choice of parameters. The points represent the digitized experimental spectrum. (A) "Good" fit generated with parameters in Table I. (B) Least-squares-generated fit. For C–F, the solid line represents a change in the specified parameter of +10% from the value in Table I and the dashed line represents a change of −10%: (C) S_M; (D) $\bar{\nu}_M$; (E) S_L; (F) $\nu_{1/2}$.

termination of excited-state molecular structure in solution should be feasible in the future.

Acknowledgments are made to the National Science Foundation (Grant No. CHE-8108451) and to the Robert A. Welch Foundation (Grant No. F733) for support of the work at The University of Texas at Austin and to the Department of Energy (Grant No. DAAG29-82-K-0111) for the work carried out at The University of North Carolina, Chapel Hill.

Appendix

Expressions of the form of eq 1 and 2 for generating line shapes are known[38] and can be derived based on a relatively straightforward Franck–Condon analysis of vibronic band intensities. The bandshape equations are expressed as $I_{v_M v_L}(\bar{\nu}) = I_{n_M n_L}(\bar{\nu})/I_{00}$, that is, as the intensity of the $v_M^* = 0$, $v_L^* = 0$ to $v_M = n_M$, $v_L = n_L$ transition relative to the intensity of the $v_m^* = 0$, $v_L^* = 0$ to $v_M = 0$, $v_L = 0$ transition, the so-called 0–0 transition. v_M and v_L are vibrational quantum numbers for two different normal modes as described in the text and an asterisk denotes a vibrational level of the excited state. The expression for the intensity of emission from v^* to v is given[39] by

$$I_{v,v^*}^{em} = \frac{64}{3}\pi^4 c N_{v^*} \nu_{v,v^*}^4 |R_e|^2 \prod_j |\langle \chi_{j,v} | \chi_{j,v^*} \rangle|^2 \qquad (A1)$$

where c is the speed of light and N_{v^*} is the number of molecules in the v^* vibrational level of the excited state. ν_{v,v^*} is the frequency of emitted light and corresponds to the energy difference between v^* and v, $\nu_{v,v^*} = (E_{v^*} - E_v)/h$. $|R_e|$ is the electronic transition moment, $R_e = \langle \psi_e | \sum_i e\vec{r}_i | \psi_e^* \rangle$, where the ψ_e are pure electronic wave functions. The $\chi_{j,v}$ are the vibrational wave functions for normal mode j corresponding to vibrational quantum number v. It follows that

$$I_{v,v^*} = \frac{I_{v,v^*}^{em}}{I_{00}} = \left(\frac{\bar{\nu}_{v,v^*}}{\bar{\nu}_{00}}\right)^4 \prod_j \frac{|\langle \chi_{j,v} | \chi_{j,v^*} \rangle|^2}{|\langle \chi_{j,0} | \chi_{j,0} \rangle|^2} \qquad (A2)$$

where $\bar{\nu}_{n,n^*} = h\nu_{n,n^*}$. As noted in the body of the paper only two modes ($j = 2$) generally need be included to obtain good fits, although they may represent averaged contributions from more than one mode. Since the emission measurements are made at low temperature (77 K), $v^* = 0$ for both modes (for $\bar{\nu}_L = 400$ cm^{-1} the population of $v_L = 1$ at 77 K is less than 0.06%) and $\bar{\nu}_{v,v^*} = \bar{\nu}_{00} - v_M\bar{\nu}_M - v_L\bar{\nu}_L$.

The form of the $(v^* = 0) \rightarrow v$ Franck–Condon factor is given[38b] in eq A3, where S_n was defined in the text.

$$|\langle \chi_{n,v} | \chi_{n,0} \rangle|^2 \propto \frac{(S_n^v)}{v!} \exp(-S_n) \qquad (A3)$$

Equation A3 is exactly correct only in the linear coupling limit, wherein the vibrational frequencies are the same in the ground and excited states. For the compounds in this study, the time-resolved resonance Raman frequencies differ by less than 10% between the ground and excited states and errors introduced by this degree of quadratic coupling are expected to be small.[38]

Equation 4A thus represents a line intensity relative to the 0–0

$$I_{v_M,v_L} = \left(\frac{\bar{\nu}_{00} - v_M\bar{\nu}_M - v_L\bar{\nu}_L}{\bar{\nu}_{00}}\right)^4 \left(\frac{S_M^{v_M}}{v_M!}\right)\left(\frac{S_L^{v_L}}{v_L!}\right) \qquad (A4)$$

line. To include the broadening effect of solvent, each line is broadened into a Gaussian distribution of intensities centered at $\bar{\nu}_{v,v^*}$ with a normalization factor of 4 ln 2 added to ensure that the integrated area corresponds to the intensity of the line. The Gaussians for each line are assumed to have the same full width at half-maximum, $\bar{\nu}_{1/2}$. Finally, to generate the complete spectrum, summations must be made over the contributions from each v_L and v_M level in the ground state, giving

$$I(\bar{\nu}) = \sum_{v_M=0}^{\infty} \sum_{v_L=0}^{\infty} \left(\frac{\bar{\nu}_{00} - v_M\bar{\nu}_M - v_L\bar{\nu}_L}{\bar{\nu}_{00}}\right)^4 \left(\frac{S_M^{v_M}}{v_M!}\right) \times \left(\frac{S_L^{v_L}}{v_L!}\right) \exp\left[-(4 \ln 2)\left(\frac{\bar{\nu} - \bar{\nu}_{00} + v_M\bar{\nu}_M + v_L\bar{\nu}_L}{\bar{\nu}_{1/2}}\right)^2\right] \qquad (A5)$$

which is equivalent to eq 1 and 2 in the text.

The actual fitting of the spectrum was accomplished by digitizing the measured spectrum (typically 75 points) and converting it to an abscissa linear in energy as noted in the Experimental Section. The initial guesses at parameters were determined as follows: (1) $\bar{\nu}_{00}$ was taken as the value of energy higher than $\bar{\nu}(I_{max})$, where the intensity was ~50% of I_{max}; (2) $\bar{\nu}_M$ was taken as 1350 cm^{-1}, a typical average frequency for the symmetric bipyridine ring stretching modes; (3) $\bar{\nu}_L$ was taken to be 400 cm^{-1} as an estimated average value for the M–N(bpy) stretching modes; (4) S_M was initially estimated by using the relationship $S_M \simeq (I_{0,1}/I_{0,0})(\bar{\nu}_{0,0}/\bar{\nu}_{0,1})^4$; (5) S_L was assumed to be ~ S_M + 1.0; (6) $\bar{\nu}_{1/2}$ was taken to be 650 cm^{-1}. With these initial parameters the spectrum was calculated by eq A5 and compared to the experimental spectrum. In actual practice each spectrum was normalized so that $I_{max} = 1.0$. The summations in eq A5 were taken from $v = 0$ to $v = 10$ since contributions from higher vibrational levels were negligible as evidenced by the magnitude of the Franck–Condon factors.

Following the initial estimate, the parameters were varied slightly, with the following criteria being used to determine the sense of the variation from experience: (1) $\bar{\nu}_{00}$ was varied to change the position of the first vibronic component on the energy scale; (2) $\bar{\nu}_M$ was varied to adjust the spacings between vibrational components; (3) changes in S_M primarily affected the relative intensities of each component; (4) $\bar{\nu}_{1/2}$ was varied to obtain the best fit to the leading edge of the spectrum; (5) variations in S_L and $\bar{\nu}_L$ primarily affected the resolution of the vibronic structure. By following these guidelines, the parameters were varied and the procedure was repeated until a "good fit" was attained. A "good fit" was defined by the correspondence of the experimental and calculated spectra, with special emphasis on (1) relative peak intensities, (2) the spacings between vibrational components, and

(38) (a) Lin, S. H.; Colangelo, L. J.; Eyring, H. *Proc. Natl. Acad. Sci. U.S.A.* **1971**, *68*, 2135. (b) Ballhausen, C. J. "Molecular Electronic Structures of Transition Metal Complexes", McGraw-Hill: New York, 1979. (c) Yersin, H.; Otto, H.; Zink, J. I.; Gliemann, G. *J. Am. Chem. Soc.* **1980**, *102*, 951. (d) Wilson, R. B.; Solomon, E. I. *Ibid.* **1980**, *102*, 4085.

(39) Herzberg, G. "Molecular Spectra and Molecular Structure. I. Spectra of Diatomic Molecules", 2nd ed.; Van Nostrand Reinhold: New York, 1950.

(3) the leading edges (high $\bar{\nu}$ values). From experience, this procedure resulted in fits that were not as well fit at low energies as at higher energies. However, in the low-energy region anharmonicity effects and errors arising from truncation of the sums in eq A5 are enhanced and as a consequence the deviations at low energies do not appear to affect in a serious way the values of the parameters derived from the spectral fits.

Attempts at nonlinear least-squares fitting of the spectra using published procedures[40] were generally unsuccessful. Problems appear to arise because the parameters are not entirely independent in that variations in one parameter may necessitate rather large changes in the others and because it is difficult to devise an algorithm that allows a computer to decide on quality of fit based, for example, on the criteria described above. The procedure that we have followed has been to examine the calculated spectrum after each iteration and, on the basis of how well it fits, choose the parameters for the next iteration. The procedure was repeated until a "good fit" (as defined above) was obtained. Standard deviations for each parameter were calculated by using the "good-fit" parameters in a nonlinear least-squares program, constrained to 0 iterations (immediate convergence). The validity of the approach lies in the consistency of the results. It should be noted that by now the approach described here has been used by a number of people who without previous knowledge of the "correct" parameters have all arrived at essentially the same values. As an illustration, in Figure 6 are shown the "good" fits for $Os(bpy)_3^{2+}$, the least-squares-generated fit, and fits obtained by varying S_M, $\bar{\nu}_M$, S_L, and $\bar{\nu}_{1/2}$ by ±10%. Clearly, Figure 6A is the best fit and it provided the parameters used in the text.

(40) Johnson, K. J. "Numerical Methods in Chemistry"; Marcel Dekker: New York, 1980.

Registry No. $Os(bpy)_3^{2+}$, 23648-06-8; $Os(bpy)_2(P_2)^{2+}$, 75441-74-6; $Os(bpy)(P_2)_2^{2+}$, 89711-31-9; $Ru(bpy)_3^{2+}$, 15158-62-0; $Ru(bpy)_2(en)^{2+}$, 47597-15-9; *fac*-Re(bpy)$(CO)_3$Cl, 55658-96-3.

Synthesis, Proton NMR Spectroscopy, and Structural Characterization of Binuclear Ruthenium Porphyrin Dimers

James P. Collman,*† Craig E. Barnes,† Paul N. Swepston,‡ and James A. Ibers*‡

Contribution from the Departments of Chemistry, Stanford University, Stanford, California 94305, and Northwestern University, Evanston, Illinois 60201.
Received August 4, 1983

Abstract: The binuclear Ru(II) porphyrin dimers $(Ru(OEP))_2$ and $(Ru(TPP))_2$ (OEP = 2,3,7,8,12,13,17,18-octaethylporphyrinato; TPP = 5,10,15,20-tetraphenylporphyrinato) have been synthesized by the vacuum pyrolysis of the mononuclear bis(pyridine) complexes $Ru(OEP)(py)_2$ and $Ru(TPP)(py)_2$ (py = pyridine). A detailed analysis of the paramagnetic shifts observed in the ^1H NMR spectra is presented, and a new model for referencing dipolar shifts in a dimeric porphyrin structure type is described. The calculated contact shifts exhibit π symmetry and indicate that the dominant mode of spin transfer into the porphyrin ring is derived from P $3e(\pi) \rightarrow$ Ru charge transfer. In addition, the crystal structure of the OEP dimer is reported. $(Ru(OEP))_2$ crystallizes as the dipentane solvate in space group C_{2h}^6-$C2/c$ with $Z = 8$ in a unit cell of dimensions $a = 27.989$ (11) Å, $b = 27.255$ (12) Å, $c = 17.737$ (8) Å, and $\beta = 102.50$ (2)°. The final agreement indices, based on 767 variables and 9806 unique intensities collected at −103 °C on an automatic diffractometer, are $R(F^2) = 0.066$ and $R_w(F^2) = 0.124$. The conventional R index on F for 7304 reflections having $F^2 > 3\sigma(F_o^2)$ is 0.042. The distance between the Ru atoms is 2.408 (1) Å and the mean Ru–N distance is 2.050 (5) Å. Each Ru atom is situated 0.30 Å out of a plane defined by four coordinating N atoms in the direction of the other Ru atom. The two porphyrin macrocycles are twisted 23.8 (1)° with respect to each other. Both porphyrinato cores have domed-type distortions with average deviations from the least-squares planes of 0.07 and 0.10 Å and maximum deviations of 0.19 and 0.24 Å, respectively. The X-ray and NMR results are consistent with a qualitative MO diagram that suggests a formal Ru–Ru bond order of 2.

Investigations into the chemistry of ruthenium porphyrins have, until now, been narrowly focused. This is surprising in view of the interesting and highly diversified chemistry that iron porphyrins are known to exhibit.[1] One factor in explaining this difference is the lack of easily prepared ruthenium(II) porphyrin complexes that do not contain the coordinatively inert carbonyl ligand. The carbonyl ligand is known to back-bond so strongly to ruthenium porphyrins that it exerts an overwhelming influence on the chemistry of these complexes.[2] Thus it is of great interest to develop new synthetic entries into ruthenium porphyrin chemistry that either bypass the carbonyl adduct or effectively utilize it to form complexes having more interesting ligands.

Two methods of removing the carbonyl ligand have been reported. Hopf et al.[3] were first to describe the photochemical ejection of CO from ruthenium porphyrins to produce a ruthenium(II) bis(pyridine) complex. Although this reaction proceeds in good yield, it is difficult to exchange cleanly the bound pyridine groups for more weakly binding ligands. In addition, a photolysis of this type is limited to those ligands that can withstand prolonged exposure to intense UV irradiation.

Recently, we[4] and others[5] described an oxidative method for removing the carbonyl ligand. The reaction of a ruthenium(II) porphyrin, Ru(P)(CO)L,[6] with *tert*-butyl hydroperoxide gives an

† Stanford University.
‡ Northwestern University.

(1) Scheidt, W.; Reed, C. *Chem. Rev.* **1981**, *81*, 543–555.
(2) Brown, G.; Hopf, F.; Meyer, T.; Whitten, D. *J. Am. Chem. Soc.* **1975**, *97*, 5385–5390.
(3) Hopf, F. R.; O'Brien, T.; Scheidt, W.; Whitten, D. *J. Am. Chem. Soc.* **1975**, *97*, 277–281.
(4) Collman, J. P.; Barnes, C. E; Collins, T. J.; Brothers, P. J.; Gallucci, J.; Ibers, J. A. *J. Am. Chem. Soc.* **1981**, *103*, 7030–7032.
(5) Masuda, H.; Taga, T.; Osaki, K.; Sugimoto, H.; Mori, M.; Ogoshi, H. *J. Am. Chem. Soc.* **1981**, *103*, 2199–2202.
(6) Abbreviations used: P = porphyrinato dianion in general; OEP = 2,3,7,8,12,13,17,18-octaethylporphyrinato; TPP = 5,10,15,20-tetraphenylporphyrinato; TTP = 5,10,15,20-tetra-*p*-tolylporphyrinato; T-*n*-PrP = 5,10,15,20-tetra-*n*-propylporphyrinato; H_{meso} = meso protons of OEP; H_β = β-pyrrolic protons of a TPP type porphyrin; H_o, $H_{o'}$, H_m, $H_{m'}$, H_p, $H_{p\text{-}CH_3}$ = ortho, ortho', meta, meta', para, para-methyl substituents on a meso phenyl ring for which the "top" and "bottom" of the phenyl rings are chemically distinct; py = pyridine; MO = molecular orbital; AO = atomic orbital; L = axial ligand in general; Me_4Si = tetramethylsilane.

0002-7863/84/1506-3500$01.50/0